Steel and Composite Structures, Vol. 8, No. 1 (2008) 1-18
DOI: http://dx.doi.org/10.12989/scs.2008.8.1.001

Analysis of restrained steel beams subjected to heating and cooling Part I: Theory

Guo-Qiang Li† and Shi-Xiong Guo

Department of Structural Engineering, Tongji University, 1239 Siping Road, Shanghai 200092, P. R. China

(Received August 8, 2007, Accepted October 22, 2007)

Abstract. Observations from experiments and real fire indicate that restrained steel beams have better fire-resistant capability than isolated beams. Due to the effects of restraints, a steel beam in fire condition can undergo very large deflections and the run away damage may be avoided. In addition, axial forces will be induced with temperature increasing and play an important role on the behaviour of the restrained beam. The factors influencing the behavior of a restrained beam subjected to fire include the stiffness of axial and rotational restraints, the load type on the beam and the distribution of temperature in the cross-section of the beam, etc. In this paper, a simplified model is proposed to analyze the performance of restrained steel beams in fire condition. Based on an assumption of the deflection curve of the beam, the axial force, together with the strain and stress distributions in the beam, can be determined. By integrating the stress, the combined moment and force in the cross-section of the beam can be obtained. Then, through substituting the moment and axial force into the equilibrium equation, the behavior of the restrained beam in fire condition can be worked out. Furthermore, for the safety evaluation and repair after a fire, the behaviour of restrained beams during cooling should be understood. For a restrained beam experiencing very high temperatures, the strength of the steel will recover when temperature decreases, but the contraction force, which is produced by thermal contraction, will aggravate the tensile stresses in the beam. In this paper, the behaviour of the restrained beam in cooling phase is analyzed, and the effect of the contraction force is discussed.

Keywords: fire-resistance; steel structure; catenary action.

1. Introduction

The aim of fire-resistance design of building structures is to avoid severe damage or collapse during fire attack. Due to the difficulty to determine global stability of a building structure subjected to fire, most Codes and Standards in the world for fire-resistance of structures adopt isolated member capacity checking. With the progress of recent research on fire-resistance of structures, more and more investigators become doubtful of the effectiveness of this method, since they have recognized, for example, that the behaviour of a steel beam in a building structure is not the same as that of an isolated beam.

Before 1990, most research studies on fire-resistant steelwork are focused on isolated members, including columns and simply-supported beams. In the 1990s, the Broadgate fire in London provided some interesting observations (SCI 1991). In the investigation of the fire, it was found that the steel beams in the structure had better fire-resistant capacity than the isolated beams in the standard fire tests.

†Corresponding author, E-mail: gqli@mail.tongji.edu.cn

In the famous fire experiments on the full-scale 8-storey steel building in Cardington, similar phenomena were observed (Wang 2002). In the experiments, some steel beams kept sustaining loads with very large deflections even when the steel temperature reached 900ºC (Fig. 1). However another noticeable fact is the damages to the beam to column connections, which is assumed to be mainly caused by the enormous axial tensile forces in the steel beams during cooling. The same phenomena were also found in the fire accident of a tall steel building in TaiPei Science and Technology Park (Fig. 2). According to observations from fire tests and actual fire accidents, the following two points on the behaviour of steel beams in a complete structure subjected to fire can be drawn:

(1) A steel beam in a structure has better fire-resistant ability than an isolated beam because of the restraints at the ends of the beam applied by the adjacent members.

(2) Tension force may be induced in the restrained beam, which is unfavorable to the connections linking the beam to the adjacent members.

In order to understand the behaviour of restrained steel beams at elevated temperatures, many experimental and theoretical studies have been carried out. Li and Jiang (2000) conducted a fire experiment on axially restrained steel beams, and noticeable axial forces in the beam were measured. Liu *et al.* (2002) investigated the effect of restraints on steel beams through fire experiments, and pointed out that the restraining effect

Fig. 1 Large deflections of restrained beams in Cardington experiments

Fig. 2 Damages to the connections in TaiPei Science and Technology Park

is important on the behaviour of the beam in fire condition. Huang & Tan (2002) and Yin & Wang (2004) analyzed restrained steel beams using finite-element methods. A simplified method is proposed by Yin and Wang (2005a, 2005b) to predict the behaviour of restrained steel beams subjected to fire. However, according to the assumption employed by Yin and Wang (2005a), the development of the yield initiation of the beam to the full yielding is ignored. On the other hand, with deflection increasing, the axial stiffness of the restrained beam subjected to fire will be gradually reduced, while this is ignored by Yin and Wang.

When a fire goes out, temperature will decrease to the ambient temperature gradually. El-Rimawi *et al*. (1996) and Bailey *et al*. (1996) investigated strain reversal and the behaviour of steel beams without axial restraints during the cooling phase. However, they paid no attention to the cooling stage of restrained steel beams after fire. In fact, contraction forces will be induced in the restrained beam when its temperature decreases. Due to the effect of the contraction force, the beam to column connection may be damaged.

Based on the previous research achievements, the behaviour of restrained steel beams subjected to heating and cooling is studied in this paper. The effects of temperature gradient in the cross-section of the beam, the stiffness of the axial and rotational restrains, and the load types on the beam are considered. A practical method for analyzing the behaviour of the restrained steel beam is proposed.

2. The behaviour of restrained steel beams subjected to increasing temperature

2.1 Features of a restrained steel beam in fire

In this paper, the study is focused on symmetrically loaded H-shaped steel beams under fire condition with axial and rotational restraints at the ends. A typical restrained beam is shown in Fig. 3, in which k_{a1} and k_{a2} are the stiffness of the axial restraints at ends, and k_r is the stiffness of the rotational restraint.

Because of the reduction in the elastic modulus, E, of steel and large plastic strains in the beam under fire condition, very large deflections exceeding 1/20 of the beam span can be produced. Fig. 4 shows the development of deflections of a restrained beam subjected to fire. With the temperature and deflection increasing, a compressive force followed by a tension force may develop in the restrained beam, as shown in Fig. 5. It can be found that the run away deflection will not occur in the restrained beam when the beam yields, and the rate of deflection is slowed down when the tension force develops in the beam.

The behaviour of a restrained beam subjected to increasing temperature can be divided into 4 stages according to the change in the axial force, as shown in Fig. 5. In stage I, the beam is elastic. In stage II, the beam goes into plastic with an axial force in compression. In stage III, the beam is plastic with an axial force in tension. In stage IV, the axial tension force in the beam reaches the maximum and then begins to decrease with the reduction of the strength of steel.

2.2 Non-uniform temperature distribution and its effect on restrained steel beam

For a beam in fire condition, the temperature distribution along the length is supposed to be uniform. According to the experimental results of Liu *et al*. (2002), the temperature distribution in the cross-section may be approximated as shown in Fig. 6. The temperature of the web and the bottom flange is T_b, and the temperature of the top flange is T_t. Generally, T_t is less than T_b.

The average temperature in the beam can be determined by:

$$T = [(A_w + A_f)T_b + A_fT_t]/A \tag{1}$$

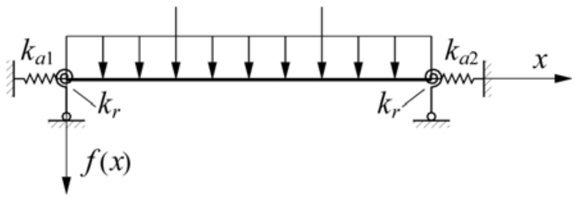

Fig. 3 Model of the restrained beam

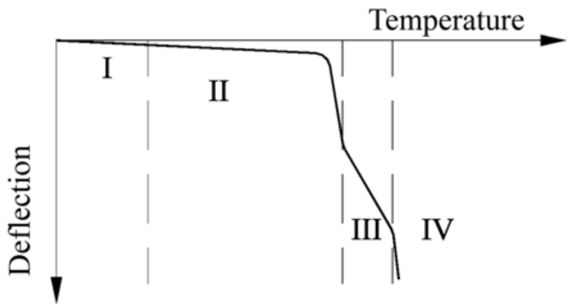

Fig. 4 Development of deflection of a restrained beam

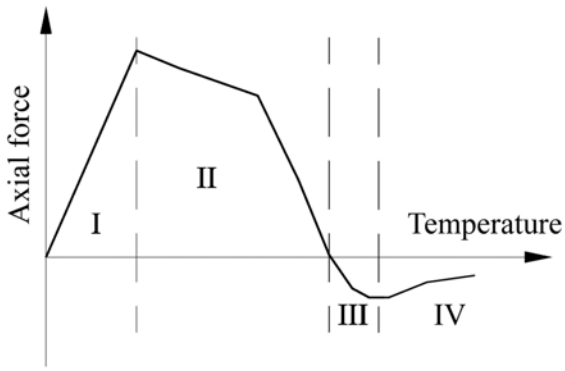

Fig. 5 Development of axial force in a restrained beam

where A_w is the area of the web; A_f is the area of the flange and A is the cross-sectional area of the beam.

For a beam without axial restraint, the thermal elongation of the beam can be expressed as:

$$\Delta L_T = \alpha TL \tag{2}$$

where α is the coefficient of thermal expansion and L is the length of the beam.

For a beam without rotational restraints at the ends, the beam will deform due to temperature gradient. For the beam with temperature distribution shown in Fig. 6, the curvature induced by the temperature gradient can be approximately determined by:

$$\phi_T = \frac{\alpha(T_b - T_t)}{h} \tag{3}$$

where h is the height of the cross-section of the beam.

The thermal bowing deflection of the beam induced by the temperature gradient can then be

Fig. 6 Assumed cross-section distribution of temperature

expressed as:

$$f_T(x) = -\frac{\alpha(T_b - T_t)}{2h}(x^2 - Lx) \tag{4}$$

And the maximum deflection at the mid-span of the beam can be determined by

$$\delta_T = \frac{\alpha(T_b - T_t)L^2}{8h} \tag{5}$$

For a beam with rotational restraints, the deflection induced by temperature gradient will be reduced due to the rotational restraints, which can be determined by:

$$\delta_T = \left(1 - \frac{k_{e,r}}{E_T I/L}\right)\frac{\alpha(T_b - T_t)L^2}{8h} \tag{6}$$

where $k_{e,r}$ is the effective rotational stiffness of the restrained beam and can be determined by Eq. (7); E_T is the elastic modulus of the steel at temperature T; and I is the second moment of inertia of the beam.

For a beam with rotational restraints, assume the stiffness of the rotational restraint to be k_r, and the rotational stiffness of the beam to be EI/L. If one of the ends is fully restrained and the other end is free, as shown in Fig. 7, under the action of M at the free end, the rotation of the end is θ. The effective rotational stiffness of the restrained beam can be expressed by $k_{e,r}=M/\theta$ and obtained by:

$$\frac{1}{k_{e,r}} = \frac{2}{k_r} + \frac{L}{E_T I} \tag{7}$$

Obviously, for beams with full rotational restraints, the effective rotational stiffness $k_{e,r}$ will be $E_T I/L$.

2.3 Deflection curve of restrained beam under fire condition

The total deflection of a restrained beam under fire condition consists of the mechanical deflection $f_m(x)$ and the temperature deflection $f_T(x)$. The deflection curve of the beam can be expressed as:

$$f(x) = f_m(x) + f_T(x) \tag{8}$$

For a beam in fire condition, when it is in elastic state, it is easy to obtain the mechanical deflection. However for a beam with large deflections, because the beam has yielded, it is difficult to formulate the

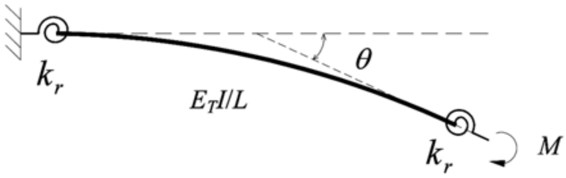

Fig. 7 Effective rotational stiffness of restrained beam

mechanical deflection. In this paper, the profile of the mechanical deflection in large deflection state is supposed to be similar to that in the elastic state, and the deflection curve of the beam in the plastic state may be obtained by the following method.

If the beam is in elastic state at ambient temperature, as shown in Fig. 8, suppose $y = f_m(x)$ and ignore the axial force, the following equation can be obtained according to the equilibrium of the moments in the beam

$$EI\frac{d^2 f_m(x)}{dx^2} + M_{end} + M_{eff}(x) + Q(x) \cdot x = 0$$

$$M_{end} = k_r \frac{df_m(x)}{dx}\bigg|_{x=0} \tag{9}$$

where M_{end} is the applied moment at the ends; $M_{eff}(x)$ is the moment about the end A induced by the applied load on the beam; and $Q(x)$ is the shear force at x position.

The mechanical deflection of the beam, $f_m(x)$, in elastic state can be obtained by solving the above differential equation. Generally, it can be expressed as:

$$f_m(x) = p \cdot g(x) \tag{10}$$

where p is a factor relevant to the applied load on the beam.

The maximum deflection of the beam is at the middle span, and the value can be determined by

$$\delta_m = f_m\left(\frac{L}{2}\right) = p \cdot g\left(\frac{L}{2}\right) \tag{11}$$

Then the load factor p can be expressed as:

$$p = \frac{\delta_m}{g\left(\frac{L}{2}\right)} \tag{12}$$

Substituting Eqs. (12) into Eq. (10), the mechanical deflection of the beam can be expressed as:

$$f_m(x) = \frac{\delta_m}{g\left(\frac{L}{2}\right)} g(x) \tag{13}$$

Considering Eq. (4) and (5), the total deflection at the middle span can be expressed as:

$$\delta = \delta_m + \delta_T \tag{14}$$

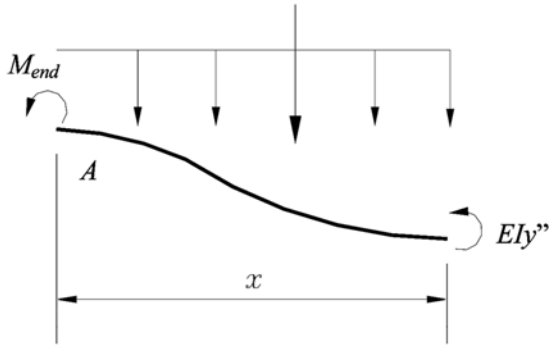

Fig. 8 Beam in elastic state at ambient temperature

2.3 Effective axial restraints and internal axial force of the beam

For the restrained beam as shown in Fig. 3, if the deflection is small, the axial stiffness in the beam can be determined by:

$$k_{bT} = \frac{E_T A}{L} \tag{15}$$

However, if the deflection of the beam is very large, the effect of deflection on the axial stiffness of the beam must be considered. Since it is very difficult to determine the accurate axial stiffness of the beam, the following approach is proposed for determining the approximate axial stiffness of the beam.

For a simply supported and curved beam shown in Fig. 9(a), the horizontal displacement of the end of the beam under the action of a horizontal force, *P*, can be determined by:

$$\Delta_P = P\int_0^l \frac{\sqrt{1+f'(x)^2}f^2(x)}{E_T I}\,dx + \int_0^l \frac{P}{E_T A\sqrt{1+f'(x)^2}}\,dx \tag{16}$$

where $f(x)$ is the profile of the beam.

In Eq. (16), the first part is the displacement induced by the moment, and the second part is that by the axial force.

If the rotation of the beam is restrained, as shown in Fig. 9(b), the moment M_P will be induced at the ends under the axial force, *P*. If rotation of the ends of the beam is fully restrained, the rotation angle of the ends is zero. Then based on the virtual work principle, the following equation can be obtained:

$$\int_0^l \frac{M_P\,\overline{M}}{E_T I}\,ds - \int_0^l \frac{f(x)P\overline{M}}{E_T I}\,ds = 0 \tag{17}$$

where $\overline{M}$ is the virtual unit moment.

The moment M_P can be worked out through Eq. (17) and expressed as

$$M_P = \frac{P\int_0^l \sqrt{1+f'(x)^2}f(x)\,dx}{\int_0^l \sqrt{1+f'(x)^2}\,dx} \tag{18}$$

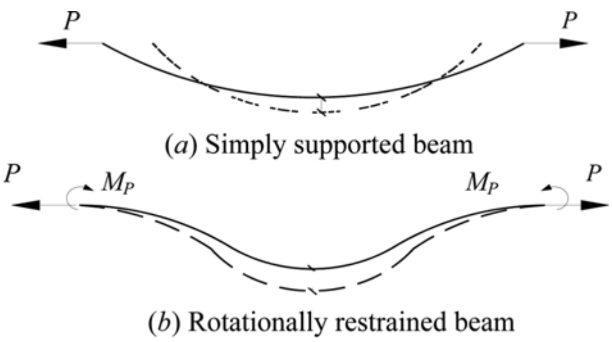

Fig. 9 The sketch of the curved beams

If the rotation of the ends of the beam is not fully restrained and the effective stiffness of the rotational restraints is $k_{e,r}$, the expression of M_p may be modified as

$$M_P = \frac{k_{e,r}}{EL/L}\frac{P\int_0^l \sqrt{1+f'(x)^2}f(x)dx}{\int_0^l \sqrt{1+f'(x)^2}dx} \tag{19}$$

Then for the rotationally restrained beam, the horizontal displacement of the ends of the beam can be determined by:

$$\Delta_P = P\int_0^l \frac{\sqrt{1+f'(x)^2}f^2(x)}{E_T I}dx + \int_0^l \frac{P}{E_T A\sqrt{1+y'^2}}dx - \frac{k_{e,r}}{EL/L}\frac{P\int_0^l \sqrt{1+f'(x)^2}f(x)dx}{\int_0^l \sqrt{1+f'(x)^2}dx}\int_0^l \frac{\sqrt{1+f'(x)^2}f(x)}{E_T I}dx \tag{20}$$

Considering the effect of deflection, the axial stiffness of the curved beam can be determined by:

$$\frac{1}{k_{bT}} = \frac{\Delta_P}{P} = \int_0^l \frac{\sqrt{1+f'(x)^2}f^2(x)}{E_T I}dx + \int_0^l \frac{1}{E_T A\sqrt{1+f'(x)^2}}dx - \frac{k_{e,r}}{EL/L}\frac{\int_0^l \sqrt{1+f'(x)^2}f(x)dx}{\int_0^l \sqrt{1+f'(x)^2}dx}\int_0^l \frac{\sqrt{1+f'(x)^2}f(x)}{E_T I}dx \tag{21}$$

For the beam in stage I, because the deflection is very small, the axial stiffness can be determined by Eq. (15). For the beam in stages II~IV, the axial stiffness can be determined by Eq. (21) approximately.

Assume the axial stiffness of the restraint at the two ends of the beam to be k_{a1} and k_{a2}. Then the effective axial stiffness of the beam is given by:

$$\frac{1}{k_{e,a}} = \frac{1}{k_{a1}} + \frac{1}{k_{bT}} + \frac{1}{k_{a2}} \tag{22}$$

The horizontal displacement of the ends of the beam due to deflection of the beam can be determined by

$$\Delta L_d = \int_0^L \sqrt{1+f'(x)^2}dx - L \tag{23}$$

Generally, Eq. (23) can be further simplified as

$$\Delta L_d = \lambda\frac{\delta^2}{L} \tag{24}$$

where λ is a factor dependent on the shape of $f(x)$.

The horizontal displacement induced by thermal expansion can be determined by Eq. (2).

Then the total displacement of the ends of the beam is:

$$\Delta L = \alpha LT - \lambda\frac{\delta^2}{L} \tag{25}$$

The internal axial force of the beam can be determined by:

$$F = \Delta L k_{e,a} \tag{26}$$

2.5 Stress distribution and the forces in the cross-section of the beam

The strain distribution in the cross-section of the beam is dependent on the curvature of the beam, ϕ_m, and the location of the neutral axis in the cross-section. The strain distribution can be sorted into three types according to the location of the neutral axis, as shown in Fig. 10, in which ε_t and ε_b are the strains of the top and bottom flanges, and a is the distance between the neutral axis and the center of the cross-section.

The mechanical curvature of the beam can be determined by

$$\phi_m = \phi_{m,m} + \phi_{m,T} = \frac{d^2 f_m(x)}{dx^2} + \frac{k_{e,r}}{EI_T/L}\frac{\alpha(T_b - T_t)}{h} \tag{27}$$

where $\phi_{m,m}$ is the curvature of $f_m(x)$; and $\phi_{m,T}$ is the curvature induced by temperature gradient.

Steel may be assumed to be an ideal elastic-plastic material with a stress-strain relationship as shown in Fig. 11. The properties of steel at elevated temperatures used in Euro code 3 (CEN 2001) are employed for this study.

The stress distribution can be classified into six types according to the three types of strain distribution and yield position, as shown in Fig. 12, where b is the minimum distance between the neutral axis and the yield zone in the cross-section.

$$b = \frac{\varepsilon_{y,T}}{\phi_m} \tag{28}$$

where $\varepsilon_{y,T}$ is yield strain at temperature T.

The axial force in the beam can be expressed as

$$F = F_w + F_f \tag{29}$$

where F_w and F_f are the forces in the web and flanges respectively.

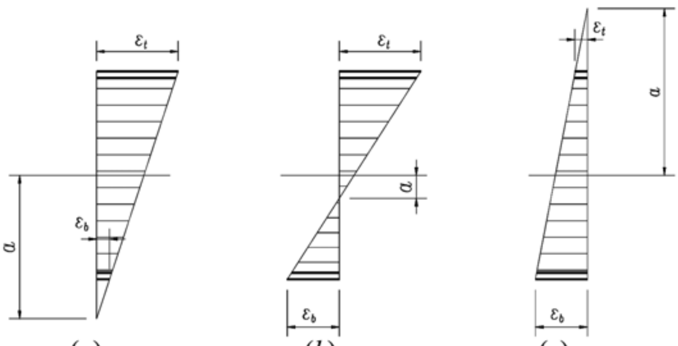

Fig. 10 Three types of distribution of strain in cross section

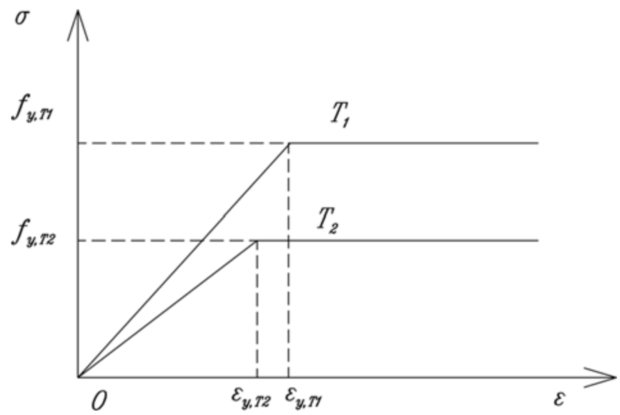

Fig. 11 Material model for steel

The moment-resistance about the center of the section can be expressed as

$$M = M_w + M_f \tag{30}$$

where M_w and M_f are the moment of the web and flanges respectively.

Assuming the stress at any point along the height of the web is $\sigma(z)$, then F_w and M_w can be determined by:

$$F_w = \int_{-\frac{h_w}{2}}^{\frac{h_w}{2}} \sigma(z) t_w dz \tag{31}$$

$$M_w = \int_{-\frac{h_w}{2}}^{\frac{h_w}{2}} \sigma(z) t_w \left(z - \frac{h_w}{2}\right) dz \tag{32}$$

where h_w is the height of the web; t_w is the thickness of the web; and z is a coordinate axis along the height of cross-section, of which the center of the cross-section is the origin.

When the beam is in elastic state, based on Eqs. (31) and (32), F_w and M_w can be given by:

$$F_w = E_{T,b} \phi A_w a \tag{33}$$

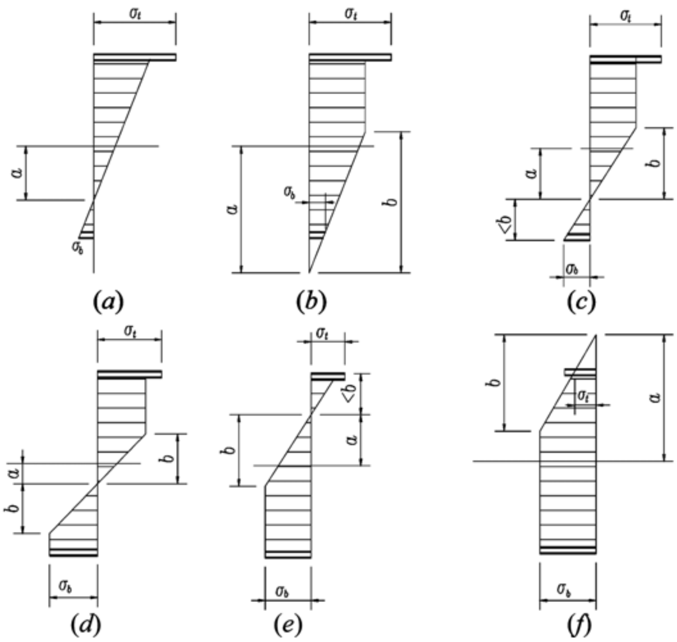

Fig. 12 Six types of distribution of stress in cross-section

$$M_w = E_{T,b} I_w \phi_m \tag{34}$$

where $E_{T,b}$ is the elastic modulus at temperature T_b; A_w is the area of the web, and I_w is the second moment of inertia of the web.

If the beam is in elastic-plastic state, then

$$F_w = \begin{cases} \frac{1}{2}\left(2a - b + h_w - \frac{(-2a + h_w)^2}{4b}\right) t_w \sigma_{y,b} & a > 0.5h_w - b \\ 2a t_w \sigma_{y,b} & |a| < 0.5h_w - b \\ \frac{1}{2}\left(2a + b - h_w + \frac{(2a + h_w)^2}{4b}\right) t_w \sigma_{y,b} & a < -(0.5h_w - b) \end{cases} \tag{35}$$

$$M_w = \begin{cases} \frac{(a - b + h_w)(-2a + 2b + h_w)^2}{24b} t_w \sigma_{y,b} & a > 0.5h_w - b \\ \left(\frac{h_w^2}{4} - a^2 - \frac{b^2}{3}\right) t_w \sigma_{y,b} & |a| < 0.5h_w - b \\ \frac{(-a - b + h_w)(2a + 2b + h_w)^2}{24b} t_w \sigma_{y,b} & a < -(0.5h_w - b) \end{cases} \tag{36}$$

where $\sigma_{y,b}$ is the yield strength of the steel at temperature T_b.

The axial force and moment-resistance of the flanges can be obtained by

$$F_f = (\sigma_b - \sigma_t)A_f \tag{37}$$

$$M_f = (\sigma_b + \sigma_t)A_f \frac{h - t_f}{2} \tag{38}$$

$$\sigma_b = \begin{cases} \sigma_{y,b} & plastic \\ E_{T,b}\phi[(h-t_f)/2 - a] & elastic \end{cases} \tag{39}$$

$$\sigma_t = \begin{cases} \sigma_{y,t} & plastic \\ E_{T,t}\phi[(h-t_f)/2 - a] & elastic \end{cases} \tag{40}$$

where σ_t and σ_b are the stresses of the top and bottom flanges; $\sigma_{y,b}$ and $\sigma_{y,t}$ is the yield strength of steel at temperature $\overline{T_b}$ and T_t; respectively t_f is the thickness of the flange; $E_{T,b}$ and $E_{T,t}$ is the elastic modulus at temperature $\overline{T_b}$ and T_t respectively.

2.6 Equilibrium equation of the beam in large deflection state

The forces on a beam in the large deflection state are shown in Fig. 13. The equilibrium equation of the beam can be expressed as

$$M_{end} + M_{mid} - M_{eff} + F\delta = 0 \tag{41}$$

where M_{end} is the moment-resistance at the end of the beam; M_{mid} is the moment resistance at the mid-span of the beam; M_{eff} is the moment about the end induced by the external load on the beam; and δ is the deflection at the mid-span of the beam.

Given the temperature distribution is determined, the iterative process solving Eq. (41) to determine the deflection of the beam is as follows:

(1) Give a trial value of δ;
(2) Calculate F by Eq. (26);
(3) Solve a from Eqs. (28)~(40) to determine the location of the neutral axis;
(4) Calculate M_{end} and M_{mid} by Eq. (30);
(5) Substitute F, δ, M_{end}, M_{mid} and M_{eff} into Eq. (41);
(6) If Eq. (41) is satisfied, the trial value of δ is the solution of the equation. If Eq. (41) is not satisfied, repeat steps (1)~(5).

Fig.14 shows the flow chart for analyzing the restrained beam subjected to increasing temperature.

3 Behaviour of restrained steel beam subjected to decreasing temperature

When the fire goes out, the steel temperature begins to decrease. When the steel temperature is

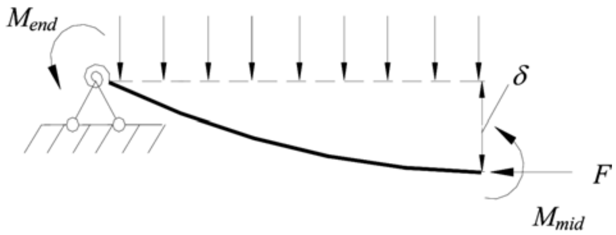

Fig. 13 Forces on a beam in large deflection state

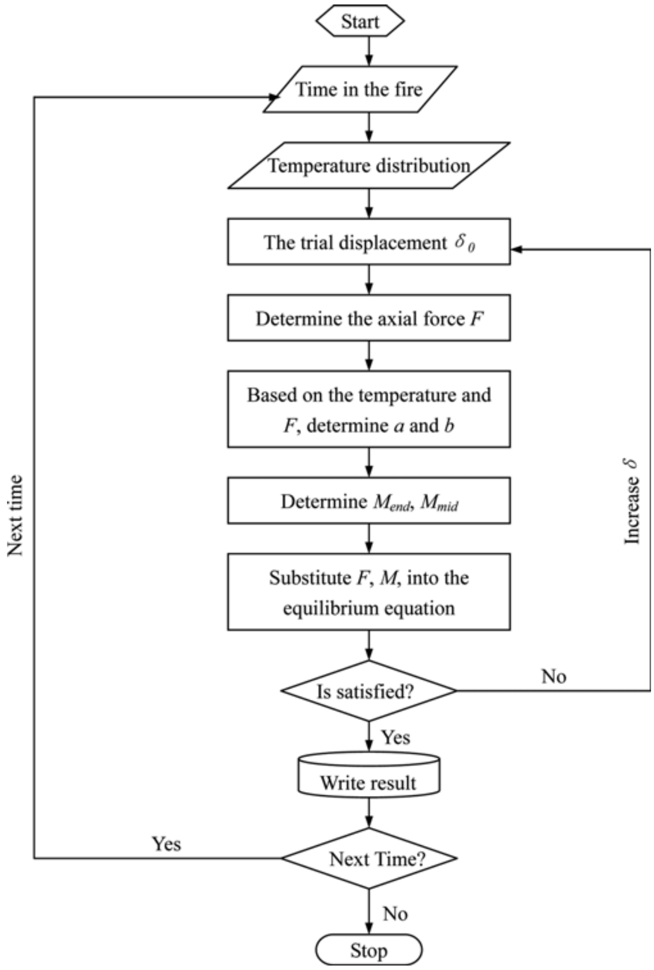

Fig. 14 The flow chart for analyzing the beam

reduced from T_1 to T_2, the elastic modulus and yield strength of steel recover, and the tensile axial force in the beam becomes $F+\Delta F$ from F because of the contraction of the beam, as shown in Fig. 15(a). During cooling, the change of thermal strain is negative and the beam will contract, as shown in Fig. 15(b). These effects will result in a net beam contraction, which will induce an additional force, ΔF, as shown in Fig. 15(c). In addition, if the decreases of the temperatures at the top and bottom flanges are different, a thermal bow deflection will be induced.

Therefore, in the analysis of the behaviour of restrained steel beams during cooling, the following factors have to be considered. The first is the recovery of the elastic modulus of steel during cooling; the second is the thermal bowing deflection induced by temperature gradient; and the third is the effect of the contraction force induced by decreasing temperature.

3.1 Deflection induced by recovery of the elastic modulus of steel

The stress-strain relation of steel when unloading is assumed to be as Fig. 16. According to the theory of El-Rimawi *et al.* (1996) about strain reversal when temperature decreases, assume the stress and strain to change as shown in Fig. 17. The plastic strain at both temperatures T_1 and T_2 is the same as ε_y. At temperature T_2, when the stress is σ_{y1}, the strain is $(\varepsilon_{T_1} - \sigma_{y1}/E_{T_1} + \sigma_{y1}/E_{T_2})$.

According to the above assumption about strain reversal during cooling, the change in deflection of the restrained beam due to recovery of the elastic modulus can be analyzed approximately by the following method, as shown in Fig. 18. At T_1, the change in mid-span deflection with the load increasing follows the track OA. Using a factor $\sigma_r s_T$ to relate the mid-span elastic deflection to the load as below:

$$\sigma_{T_1} = \frac{\delta}{p} = \frac{c_L}{E_{T_1}} \tag{42}$$

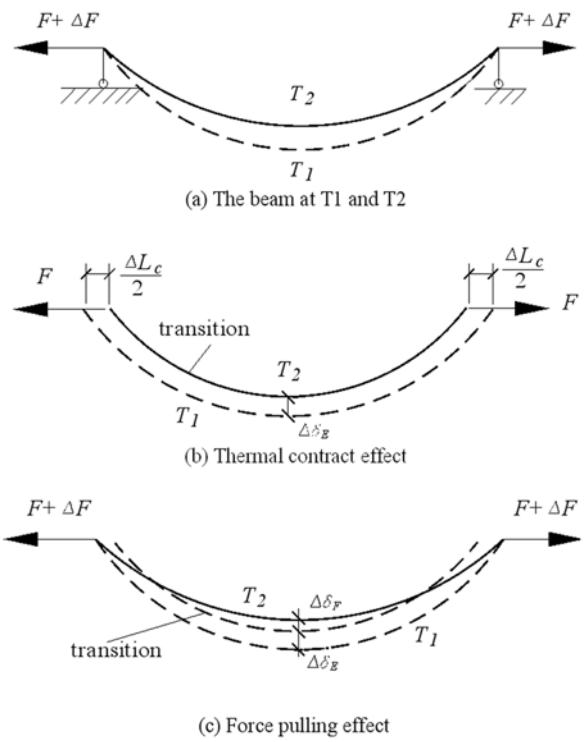

Fig. 15 Behavior of the restrained beam in cooling phase

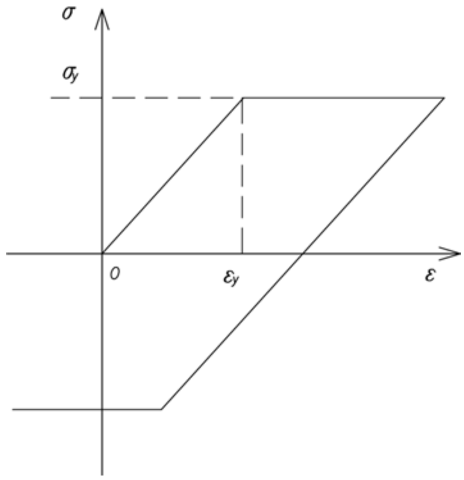

Fig. 16 Stress-strain curve of steel when unloading

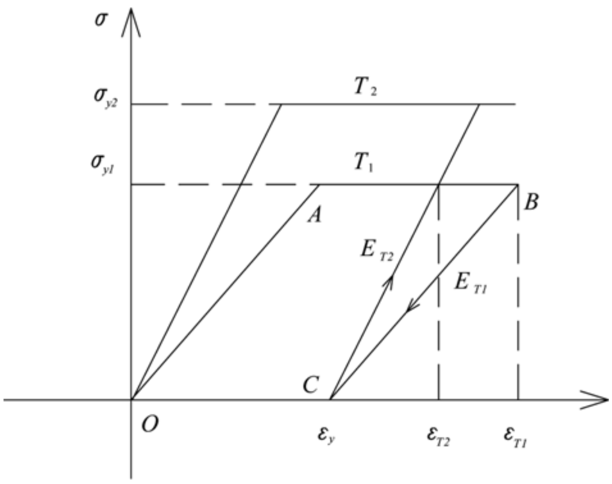

Fig. 17 Reversal of stress in cooling

where c_L is a factor dependent on the span of the beam and the type of loads on the beam.

Suppose the deflection of the beam at temperature T_1 is δ_{T_1}. When temperature decreases, if the plastic deflection is maintained, the deflection will follow the track A-C-B, as shown in Fig. 18. Then the deflection at temperature T_2 can be determined by

$$\delta_{T_2} = \delta_{T_1} - ps_{T_1} + ps_{T_2} \tag{43}$$

At ambient temperature, under the action of p, the displacement is given by:

$$\delta_0 = s_0 p = \frac{c_L}{E_0} p \tag{44}$$

According to Eqs. (42) and (44),

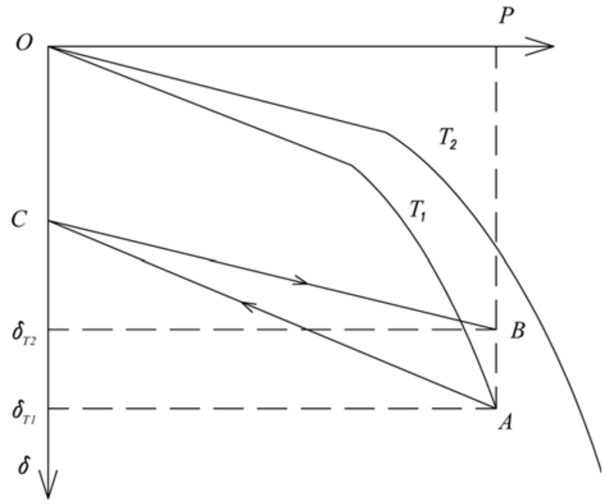

Fig. 18 Deflection reversal of restrained beam

$$ps_{T_1} = \delta_0 E_0 / E_{T_1},\ ps_{T_2} = \delta_0 E_0 / E_{T_2}$$

Thus the mid-span deflection of the beam at temperature T_2 can be determined by:

$$\delta_{T_2} = \delta_{T_1} - \delta_{rev,E} \tag{45}$$

where $\delta_{rev,E}$ is the deflection reversal induced by the recovery of the elastic modulus, which can be given by:

$$\delta_{rev,E} = \delta_0 E_0 \left(\frac{1}{E_{T_1}} - \frac{1}{E_{T_2}}\right) \tag{46}$$

If the temperatures of the bottom and top flanges of the beam are different, the following equivalent elastic modulus can be used for $E_{T_i} (i = 1,2)$

$$E_{T_i} = \frac{E_{T_{i,b}} + E_{T_{i,t}}}{2} \tag{47}$$

3.2 Deflection induced by temperature gradient in the beam during cooling

Due to decreasing temperature, the following change in temperature gradient in the beam is induced:

$$\Delta T' = \frac{(T_{2,b} - T_{1,b}) - (T_{2,t} - T_{1,t})}{h} \tag{48}$$

Using Eq. (6), the deflection reversal induced by this temperature gradient change can be determined by

$$\delta_{rev,g} = \left(1 - \frac{k_{e,r}}{E_T I / L}\right) \frac{\alpha[(T_{2,b} - T_{1,b}) - (T_{2,t} - T_{1,t})]L^2}{8h} \tag{49}$$

where $(T_{2,b} - T_{1,b})$ and $(T_{2,t} - T_{1,t})$ are respectively the temperature variations in the bottom and top flanges of the beam when temperature decreases from T_1 to T_2.

3.3 Effects of the contraction force

During decreasing temperature, the yield strength of steel recovers and an additional tensile axial force, ΔF, is generated as:

$$\Delta F = \alpha L(T_1 - T_2)k_{e,a},\ \Delta F + F \le Af_{yT_2} \tag{50}$$

A deflection reversal will also be induced by ΔF, which can be determined by

$$\delta_{rev,F} = \frac{2}{E_{T_2}I}\int_0^{\frac{L}{2}}\left(\frac{1}{2}x\right)[f(x)F_c]\sqrt{1+(f'(x))^2}dx \text{ for simply-supported beams} \tag{51a}$$

$$\delta_{rev,F} = \frac{2}{E_{T_2}I}\int_0^{\frac{L}{2}}\left(\frac{L}{8}-\frac{1}{2}x\right)[M_c - f(x)\Delta F]\sqrt{1+(f'(x))^2}dx \text{ for rotationally restrained beams} \tag{51b}$$

For a rotationally restrained beam with the effective stiffness of the rotational restraints to be $k_{e,r}$, $\delta_{rev,F}$ can be expressed as

$$\delta_{rev,F} = \frac{2}{E_{T_2}I}\int_0^{\frac{L}{2}}\left(\frac{k_{e,r}}{EI/L}\frac{L}{8}-\frac{1}{2}x\right)\left[\frac{k_{e,r}}{EI/L}M_c - f(x)\Delta F\right]\sqrt{1+(f'(x))^2}dx \tag{52}$$

3.4 Variation of deflection of the beam during cooling

In summary, when temperature descends from T_1 to T_2, the deflection of the beam will change from δ_{T_1} to δ_{T_2} as

$$\delta_{T_2} = \delta_{T_1} - \delta_{rev,E} - \delta_{rev,g} - \delta_{rev,F} \tag{53}$$

The complete behaviour of the beam during cooling phase of a fire can be analyzed incrementally, until the steel temperature returns to ambient.

3.5 Effects of the internal force in the restrained beam on beam-column connection

In Fig. 4, it can be seen that in the earlier stage of the restrained beam subjected to fire, a compressive axial force is generated. In stage III, a tensile axial force in the beam is produced by catenary action. When temperature decreases, a very large axial tension force in the beam will develop by thermal contraction of the beam. Moreover, additional bending moments at the ends of the beam will be produced by the contraction force. Under the combined effect of the contraction force and the additional bending moments, the tensile stress in the beam near the connection can be tremendous. This tensile action may cause damage in the beam-to-column connections, as found in realistic fire accidents (Fig. 1 and Fig. 2).

4. Summary

This paper has presented a theory for prediction of the complete behaviour of restrained beams in fire. Based on the assumption of plane cross-section, the strain and stress distributions in the cross-section of the beam subjected to temperature increasing and decreasing is assumed, and the axial force and bending moment can be worked out by integrating the stresses of the cross-section. By substituting the axial force and bending moment into the equilibrium equation of the restrained beam, an equation about the mid-span deflection can be obtained. By solving the equation, the development of the deflection, axial force and bending moment of the beam in fire condition can be studied.

The companion paper will present the results of a validation and parametric study.

Acknowledgment

The studies presented in this paper are sponsored by the Natural Science Foundation of China through the Outstanding Youth Project (No.59478038). The financial support from NSFC is especially acknowledged.

References

Baily, C. G., I. Burgess W. and Plank, R. J. (1996), "Analyses of the effect of cooling and fire spread on steel-framed buildings", *Fire Safety. J*, **26**(4), 273-293.

El-Rimawi, J. A., Burgess, I. W. and Plank, R. J. (1996), "The treatment of strain reversal in structural members during the cooling phase of a fire", *J. Constr. Steel Res*., **37**(2), 115-134.

European Committee for Standardization (CEN). DAFT ENV 1993-1-2, Eurocode 3: *Design of steel structures, Part 1.2* : *General rules/structural fire design*, 2001.

Huang, Z. F. and T K. H. (2002), "Structural response of a steel beam with a frame during a fire", *Proceedings of the Third International Conference on Advances in Steel Structures*, **Vol. II**, 1111-1118.

Li, G. Q., He, J. L. and Jiang, S. C. (2000), "Fire-resistant experiment and theoretical calculation of a steel beam", *China Civil Eng J*, **32**(4), 23-26.

Liu, T. C. H., Fahad, M. K. and Davies, J. M. (2002), "Experimental investigation of behaviour of axially restrained steel beams in fire", *J. Constr. Steel. Res*., **58**(9), 1211-1230.

Steel Construction Institute. (1991) *Structural Fire Engineering Investigation of Broadgate Phase 8 fire.* June, Ascot.

Wang, Y. C. (2002), *Steel and Composite Structures*: *Behaviour and Design for Fire Safety*, Spon Press, London.

Yin, Y. Z. and Wang, Y. C. (2005a), "Analysis of catenary action in steel beams using a simplified hand calculation method, Part 1 : theory and validation for uniform temperature distribution", *J. Constr. Steel. Res.*, **61**(2), 188-211.

Yin, Y. Z. and Wang, Y. C. (2005b), "Analysis of catenary action in steel beams using a simplified hand calculation method, Part 2 : validation for non-uniform temperature distribution", *J. Constr. Steel Res*, **61**(2), 213-234.

Yin, Y. Z., Wang, Y. C. (2004), "A numerical study of large deflection behaviour of restrained steel beams at elevated temperatures", *J. Constr. Steel. Res.*, **60**(7), 1029-1047.

BU